Research on multi-parametric sensors based on multi-mode microfiber*

DONG Taiji, LIU Xu, WANG Yunkai, GAO Bingkun, JIANG Chunlei, and WANG Xiufang**

College of Electrical and Information Engineering, Northeast Petroleum University, Daqing 163318, China

(Received 17 April 2023; Revised 16 July 2023)

A multi-parametric sensor based on multi-mode microfiber (MMF) is proposed, utilizing the modal interference between HE_{11} mode and HE_{12} mode in the elongated multi-mode fiber to achieve the temperature and pressure measurement. In this paper, the simulation model of modal interference based on MMF is established and the mechanism of modal interference is analyzed. Using the different mechanisms of modal response in the fiber at different wavelengths, the temperature was inverted using the offset of wavelengths in the spectrum, and the pressure was measured using the change of light intensity. The independent measurement of temperature and pressure was achieved. The experimental results show that the sensor has a temperature sensitivity of 1.305 nm/°C. In the case of pressure sensing, the sensor shows a sensitivity of −0.163 dBm/g.

Document code: A **Article ID:** 1673-1905(2024)01-0018-5

DOI https://doi.org/10.1007/s11801-024-3072-y

As a combination of fiber optics and nanotechnology, micro/nanofiber (MNF) has become an important trend in exploring optic sensing technologies, and it is clear that reducing the size of sensing structures is often a necessary step to give sensors faster response, higher sensitivity, lower power consumption and better spatial resolution, and optical ultrafine fibers are one of the best candidates to achieve this purpose[1]. In recent years, optical ultrafine fibers have become a new platform for exploring MNF technologies. Due to its excellent geometric and material uniformity, wavelength or subwavelength diameter, high refractive index contrast between the solid fiber core and the surrounding medium (e.g. vacuum, gas or liquid), MNF can be used with low optical losses, outstanding mechanical flexibility and tight optical guidance constraints and large fractional order swift fields[2-4], which gives it special advantages, such as small footprint, fast response, high sensitivity, and low power consumption, making it a versatile platform for MNF optical sensing, which is now widely used for the measurement of physical quantities, such as pressure, temperature, and vibration[5-9].

Recently, ultrafine optical fibers with diameters less than 10 μm have become extremely promising sensing platforms due to their unique transmission properties, and because the diameter of MNF is close to or lower than the wavelength of guided light, some of the guided light leaks out of the fiber in the form of a evanescent field, which is more sensitive to the external environment than the mode field inside the fiber, and researchers have reported various microfiber-based sensor schemes, including micro-gratings[10,11], interferometers[12,13], microresonators[1], and surface plasmon resonance-based microfibers[14]. Although MNF exhibits many outstanding properties, they also have some inherent limitations in terms of single measurement parameters, sensitivity and repeatability, which limit their application in sensing measurement, in addition to the cross-sensitivity between temperature and pressure during measurements, which has been a major focus for researchers. GUO et al[15] proposed a polymer nanocomposite MNF to demonstrate an optical sensor that can simultaneously detect and differentiate temperature and strain, but its sensor fabrication is more difficult and cumbersome to operate. LU et al[16] proposed a reflective fiber-optic sensor for simultaneous measurement of seawater temperature, which achieves simultaneous detection of seawater temperature and pressure by combining an MNF coupler with a Sagnac ring, using the high thermo-optical coefficient of polydimethylsiloxane (PDMS) and the high sensitivity of the evanescent field around the MNF coupler. WEN et al[17] proposed a dispersion turning point-based MNF axial stress sensor, which can reach a maximum sensitivity of 166.9 pm/με, but has a single measurement parameter and suffers from cross-sensitivity to temperature and pressure. Moreover, for the field of pipeline leak detection, simultaneous measurement of physical parameters, such as pressure in the pipeline, surrounding temperature, and pipeline vibration, is a comprehensive and effective method in pipeline leak detection. The torsion-sensitive loop integrated Mach-Zehnder interferometer (LMZI) sensor based on microfiber was proposed to achieve the extraction of the characteristic frequency of the pipeline leakage signal[18], by detecting the torque

* This work has been supported by the Joint Guidance Project of Natural Science Foundation of Heilongjiang Province, China (No.LH2022E024).

** E-mail: gaobk@163.com

change of the fiber loop when the pipeline leaks, but the sensor structure is more fragile, not easy to encapsulate, and the sensitivity is poor. In Refs.[19—21], ZHANG et al proposed a flexible wearable sensor for human health monitoring, which achieved the measurement of human temperature, fingertip pressure, pulse and other parameters, but pressure and temperature are usually mixed together, and it is very difficult to detect temperature and pressure by simply recording the output optical intensity.

In this work, an in-line Mach-Zehnder interferometer (MZI) based multi-mode microfiber (MMF) is proposed. By drawing a multi-mode fiber into a non-adiabatic fiber, the HE_{11} mode and HE_{12} mode are excited in the transition region of the MMF, and when the external environment changes, it changes the optical range difference between the two modes, which leads to a shift in the interference spectrum, thus realizing the temperature or pressure sensing. We derived the multi-mode interference theory and simulated the transmission modes in optical fiber, and analyzed the sensing mechanism of in-line MZI, which can effectively distinguish the spectral changes caused by temperature and pressure. The proposed sensor provides a new perspective to solve the cross-sensitivity of temperature and stress.

As Fig.1 shows, the structure of non-adiabatic microfiber, the waist area of MMF is connected to the non-tapered area through two mutation zones. During the transmission of light, the fundamental mode LP_{01} propagating in the non-tapered area will excite the fundamental mode HE_{11} and higher-order mode HE_{12} in the transition cone area. Due to the thin diameter of the MMF, the abrupt field of the excited mode will leak out from the fiber core, and when the external environment changes, it will change the optical range difference between the two modes, thus causing the spectrum to change. Fig.1(a) shows the three-dimensional (3D) simulation schematic of HE_{11} mode and HE_{12} mode at the incident light wavelength of 1 550 nm and the waist area diameter of 2 μm of the MMF, and Fig.1(b) gives the two-dimensional (2D) optical field simulation schematic of HE_{11} mode and HE_{12} mode. It can be seen from Fig.1 that most of the energy of HE_{11} mode is concentrated in the fiber, while a part of the energy of higher-order mode HE_{12} will leak out from the fiber core in the form of evanescent field, therefore, HE_{12} is more sensitive to the changes of the surrounding medium, as HE_{13} mode in the fiber is not effectively excited, therefore, the interference in the fiber is mainly concentrated in HE_{11} and HE_{12} modes.

Assume that I_1 and I_2 are HE_{11} and HE_{12} initial intensities, and φ is the phase difference existing between the two modes, which is related to the length L of the waist region of the MMF. The output spectral intensity can be expressed by[22]

$$I = I_1 + I_2 + 2\sqrt{I_1 I_2}\cos\varphi. \tag{1}$$

The phase φ, which causes the periodic variation of the interference spectrum, can be expressed by

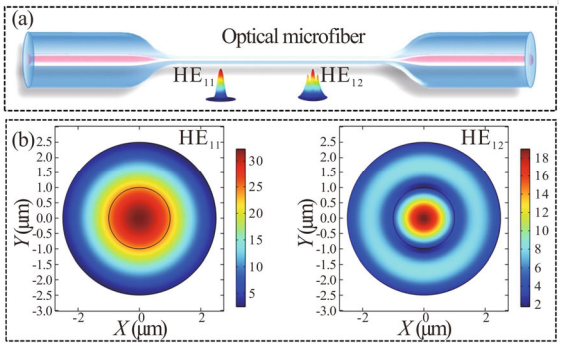

Fig.1 (a) Schematic diagram of MMF sensor structure; (b) Two-dimensional electric field distributions of HE_{11} and HE_{12} modes in an MMF with a diameter of 2 μm

$$\varphi = \Delta\beta L = \left(\Delta n_{\text{eff}} \times \frac{2\pi}{\lambda_N}\right) L = (2N-1)\pi, \tag{2}$$

where $\Delta\beta$ and Δn_{eff} represent the propagation constant difference and effective refractive index difference between HE_{11} and HE_{12} modes, respectively, and λ_N represents the wavelength of the Nth dip in the interference spectrum. The refractive index sensitivity of the dip λ_N can be calculated as

$$S=\left(\frac{\partial\lambda_N}{\partial n}\right)=\frac{\lambda_N}{n_{\text{g}}^{\text{HE}_{11}} - n_{\text{g}}^{\text{HE}_{12}}}\frac{\partial(\Delta n_{\text{eff}})}{\partial n} = \frac{\lambda_N}{G}\frac{\partial(\Delta n_{\text{eff}})}{\partial n}, \tag{3}$$

where $G = n_{\text{g}}^{\text{HE}_{11}} - n_{\text{g}}^{\text{HE}_{12}} = \Delta n_{\text{eff}} - \lambda_N \times \partial(\Delta n_{\text{eff}})/\partial\lambda_N$ represents the group effective refractive index difference between HE_{11} and HE_{12} modes, and from the above equation, S depends on λ_N, G, and $\partial(\Delta n_{\text{eff}})/\partial n_{\text{SRI}}$, but is not affected by the fiber length.

The equation for the wavelength temperature response including the thermo-optical coefficient is shown below[23]

$$\frac{\partial\lambda}{\partial T} = \frac{\lambda\left(a_2^2 n_2 L_1 S_1 + a_1^2 n_1 L_2 S_2\right)}{a_2^2 n_2 L_1 + a_1^2 n_1 L_2}, \tag{4}$$

where $S_1=\alpha_1+\xi_1$, $S_2=\alpha_2+\xi_2$, α_1, α_2, ξ_1 and ξ_2 are the thermal expansion coefficients and thermo-optical coefficients of silica and PDMS, respectively, and L_1 and L_2 are the lengths of micro-nano fiber and PDMS, respectively. When the external temperature changes, L_1, L_2, n_1, n_2 will change due to the thermal expansion effect and thermo-optical effect, which will lead to the shift of the spectrum in the spectrum. When the temperature increases, the refractive index of PDMS decreases faster than that of silica due to the higher thermo-optical coefficient of PDMS (-10^{-4} °C^{-1}). The increase in refractive index contrast leads to a red shift in the cutoff wavelength of the particular higher-order mode.

While for pressure sensing, MMF can convert the pressure stimulus to bend in the waist area, when the MMF bends, resulting in larger fiber transmission loss, part of the light will leak into the cladding, resulting in a change in output light intensity.

A non-adiabatic tapered ultrafine optical fiber was prepared by a two-step stretching method. First, the multi-mode optical fiber was stretched by the melt stretching method, and the fiber was heated with an alcohol lamp. In this step, the fiber needs to be stretched rapidly to form two abruptly tapered transition regions. Then, the middle gradually thinning waist area is further slowly thinned by heating with an alcohol lamp. During the second thinning step, we use demodulation equipment to monitor the real-time transmission spectrum of the fiber. We immediately stop the stretching when a sinusoidal reflection spectrum appears on the spectrum, at which point the diameter of the fiber girdle is about 2.13 μm. The physical diagram of the non-adiabatic micro-nano fiber is shown in Fig.2. We measured the transmission loss of the sensor using a power meter, when the input power is 12 mW, the output power of the micro-nano fiber sensor is about 9.7 mW, and the transmission loss is 0.92 dB.

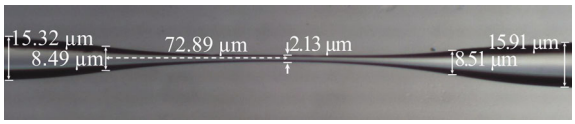

Fig.2 Physical diagram of the micro-nano fiber optic sensor

Based on the theoretical analysis in the previous section, to verify the feasibility of the scheme applied to the sensing of external environmental parameters, we conducted an experimental study with the experimental setup shown in Fig.3, which consists of a demodulation system (PXIe-4844), manufactured by NI, with a built-in broadband light source (1 510—1 590 nm), and also serves as a spectrometer to detect the reflection spectrum of MMF in real time. The module provides 1 pm wavelength accuracy, 1 pm repeatability, and 1 pm stability. The signal processing system consists of a personal computer (PC) host and associated signal processing software. The sensing unit consists of the MMF. During the experiment, we used PDMS to clad the MMF to improve the sensitivity. Since PDMS's refractive index (n≈1.40) is slightly lower than that of silica (n≈1.46), the fiber PDMS can effectively enclose the MMF and isolate the evanescent field, while maintaining the high mechanical flexibility of MMF and low optical loss.

First, we measured the temperature response curve of the sensor, we used the heating base of the 3D printer to heat the PDMS encapsulated MMF, and set the initial temperature to 26 °C. To test the sensitivity of this sensing, we chose a 1 °C step to heat the MMF, and its spectral response curve is shown below. The experimental results show that as the temperature increases, the reflection curve in the spectrum was red shifted. According to Eq.(4), this is because when the temperature around the MMF increased, it changed the refractive index distribution of the medium around the MMF, resulting in a red shift in the reflection spectrum. Furthermore, as shown in Fig.4, the amplitude of the spectral lines changes slightly with increasing temperature. In addition to the effect of refractive index, we consider that it may be due to the non-uniform thickness of the PDMS films made, resulting in a non-uniform heating during the heating process, which leads to a slight change in the amplitude of the spectral lines. Since we detected the temperature by detecting the red shift of the spectrum, we neglected the slight changes in the spectral amplitude during the temperature measurement.

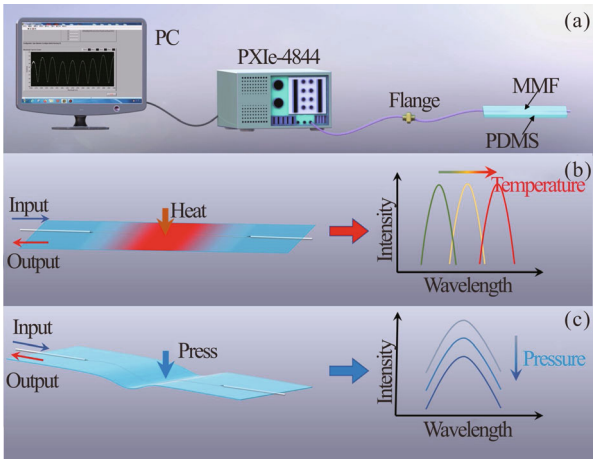

Fig.3 (a) Experimental setup for temperature and pressure sensing; (b) Schematic diagram of temperature sensing principle; (c) Schematic diagram of pressure sensing principle

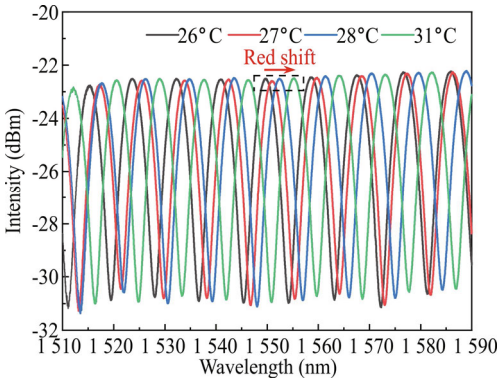

Fig.4 Temperature responses of the sensor

Furthermore, to study the relationship between the spectral offset and temperature, we set the temperature range within 26—76 °C with a step of 5 °C. We observed the spectral offset on the demodulation equipment and fitted the temperature to the wavelength, and the experimental results are shown in Fig.5, from which it can be seen that the wavelength offset increases as the temperature rises, and the offset of the spectrum is linearly related to the change of temperature. The fitted relationship is y=1.305x+1 496.756, where x represents the temperature, y represents the wavelength, and the sensitivity is 1.305 nm/°C.

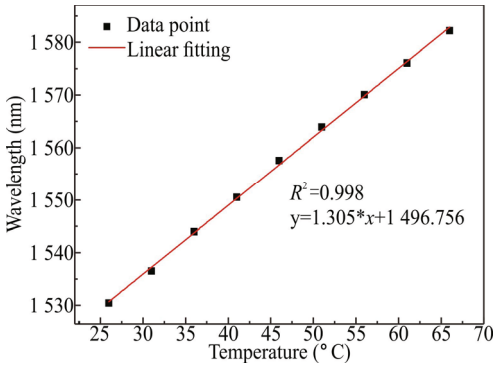

Fig.5 Relationship between temperature and wavelength

Finally, we tested the response mechanism of the sensor under different pressures. We simulated different pressures with different grams of weights, and selected 5 g and 10 g for experiment. The experimental results are shown in Fig.6. It can be seen that as the grams of weights increase, the intensity of the reflection spectrum detected at the output also changes. We think this is because when the weights act on the MMF, the bending loss becomes the main factor affecting the intensity of the reflected spectrum output. To verify this idea, we extended the range of weights and tested the output responses of MMF with 5 g, 10 g, 20 g, 50 g, and 100 g objects, and fitted the output intensities with these weights. The results are shown in Fig.7. The fitted equation is y=−0.163x−36.897, where x represents the weight and y represents the wavelength, and the sensitivity is −0.163 dBm/g.

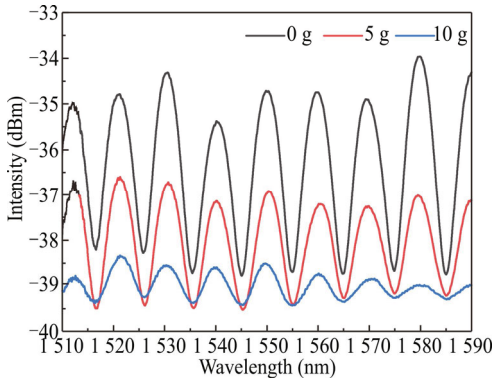

Fig.6 Pressure responses of the sensor

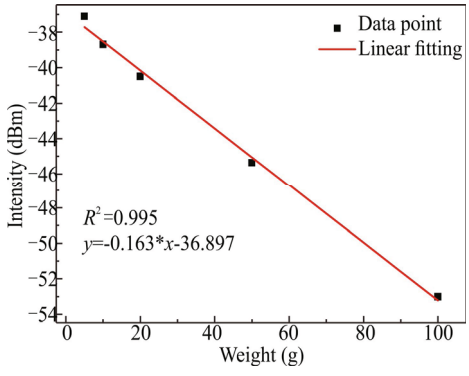

Fig.7 Output intensity variation with the weight

Finally, in order to test the stability of the sensor, we conducted the repeatability measurement experiment. We selected a weight of 5 g to conduct a repeatability test on the micro-nano fiber sensor, and the measurement results are shown in Fig.8.

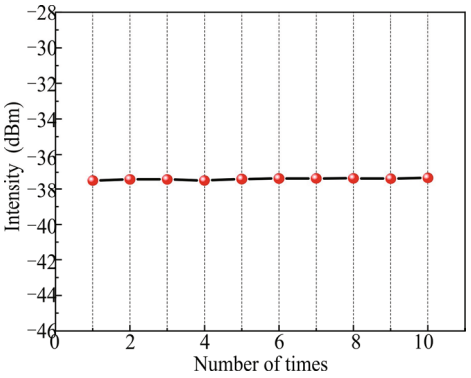

Fig.8 Repeatability measurement results

We conducted 10 measurements on the micro-nano fiber sensor, and the measurement results show that the fluctuation of the 10 measurements does not exceed 0.051 dBm, which can verify the stability of the sensor.

We designed and fabricated a multi-parametric sensor based on MMFs, and achieved independent measurement of temperature and pressure by stretching the multi-mode fiber to form an in-line MZI, utilizing the offset of the reflected spectrum for temperature sensing and the change of spectral intensity for pressure sensing. The experimental results show that the sensor has a sensitivity of 1.305 nm/°C for temperature sensing and −0.163 dBm/g for pressure sensing. The performance of the sensor has been tested at different temperatures and pressures, and the results show that the sensor has good linearity. The proposed method provides a new perspective on the independent measurement of pressure and temperature, and is expected to be applied to human wearable sensors.

Ethics declarations

Conflicts of interest

The authors declare no conflict of interest.

References

[1] TONG L. Micro/nanofibre optical sensors: challenges and prospects[J]. Sensors (Basel), 2018, 18(3): 903.

[2] LUO H, SUN Q, LI X, et al. Refractive index sensitivity characteristics near the dispersion turning point of the multimode microfiber-based Mach-Zehnder interferometer[J]. Optics letters, 2015, 40(21): 5042-5045.

[3] KAMIL Y M, ABU BAKAR M H, ZAINUDDIN N H, et al. Progress and trends of optical microfiber-based biosensors[J]. Biosensors-Basel, 2023, 13(2): 17.

[4] LUO W, CHEN Y, XU F. Recent progress in microfiber-optic sensors[J]. Photonic sensors, 2021, 11(1): 45-68.

[5] YAO N, WANG X, MA S, et al. Single optical microfiber enabled tactile sensor for simultaneous temperature and pressure measurement[J]. Photonics research, 2022, 10(9): 2040.

[6] WU Q, QU Y W, LIU J, et al. Single mode-multi mode-single mode fiber structures for sensing applications-a review[J]. IEEE sensors journal, 2021, 21(11): 12734-12751.

[7] LI G C, WANG Y J, SHI A C, et al. Review of seawater fiber optic salinity sensors based on the refractive index detection principle[J]. Sensors, 2023, 23(4): 27.

[8] SUN L P, YUAN Z, HUANG T, et al. Ultrasensitive sensing in air based on Sagnac interferometer working at group birefringence turning point[J]. Optics express, 2019, 27(21): 29501-29509.

[9] XU S, CHANG W, ZHANG Y, et al. Ultrasensitive enhanced fabrication-tolerance refractometer based on PANDA-air-hole microfiber at the birefringent dispersion turning point[J]. Optics express, 2021, 29(3): 3694-3707.

[10] CHEN X D, CHEN W H, LIU Y, et al. Sensitivity-enhanced strain sensor with a wide dynamic range based on a novel long-period fiber grating[J]. IEEE sensors journal, 2022, 22(4): 3196-3201.

[11] LI Q S, CAI L, MA Y H, et al. Research progress of biosensors based on long period fiber grating[J]. Chinese optics, 2018, 11(3): 475-502. (in Chinese)

[12] TAN Y Z, SUN L P, JIN L, et al. Long period grating-based microfiber Mach-Zehnder interferometer for sensing applications[C]//Proceedings of the 4th Conference on Asia Pacific Optical Sensors (APOS), 2013, Wuhan, China. Washington: SPIE, 2013: 8924.

[13] ZHU X J, PAN Y Q, SUN A, et al. High sensitivity curvature sensor based on a double-sphere tapered no-core fiber Mach-Zehnder interferometer[J]. Optics and laser technology, 2022, 155: 8.

[14] ZHENG W L, ZHANG Y N, LI L K, et al. A plug-and-play optical fiber SPR sensor for simultaneous measurement of glucose and cholesterol concentrations[J]. Biosensors & bioelectronics, 2022, 198: 8.

[15] GUO J J, ZHOU B Q, YANG C X, et al. Stretchable and upconversion-luminescent polymeric optical sensor for wearable multifunctional sensing[J]. Optics letters, 2019, 44(23): 5747-5750.

[16] LU J Y, ZHANG Z R, YU Y, et al. Simultaneous measurement of seawater temperature and pressure with polydimethylsiloxane packaged optical microfiber coupler combined Sagnac loop[J]. Journal of lightwave technology, 2022, 40(1): 323-333.

[17] WEN J, YAN X, GAO X, et al. Axial strain sensor based on microfiber couplers operating at the dispersion turning point[J]. IEEE sensors journal, 2022, 22(5): 4090-4095.

[18] PNG W H, LIN H S, PUA C H, et al. Pipeline monitoring and leak detection using loop integrated Mach Zehnder interferometer optical fiber sensor[J]. Optical fiber technology, 2018, 46: 221-225.

[19] JIANG C, ZHANG Z, PAN J, et al. Finger-skin-inspired flexible optical sensor for force sensing and slip detection in robotic grasping[J]. Advanced materials technologies, 2021, 6(10).

[20] ZHANG L, PAN J, ZHANG Z, et al. Ultrasensitive skin-like wearable optical sensors based on glass micro/nanofibers[J]. Opto-electronic advances, 2020, 3(3): 19002201-19002207.

[21] PAN J, ZHANG Z, JIANG C, et al. A multifunctional skin-like wearable optical sensor based on an optical micro-/nanofibre[J]. Nanoscale, 2020, 12(33): 17538-17544.

[22] ZHANG N M Y, LI K, ZHANG N, et al. Highly sensitive gas refractometers based on optical microfiber modal interferometers operating at dispersion turning point[J]. Optics express, 2018, 26(22): 29148-29158.

[23] CAI L, LIU Y, HU S, et al. Optical fiber temperature sensor based on modal interference in multimode fiber lengthened by a short segment of polydimethylsiloxane[J]. Microwave and optical technology letters, 2019, 61(6): 1656-1660.